RSC Advances

ROYAL SOCIETY OF CHEMISTRY

www.rsc.org/advances

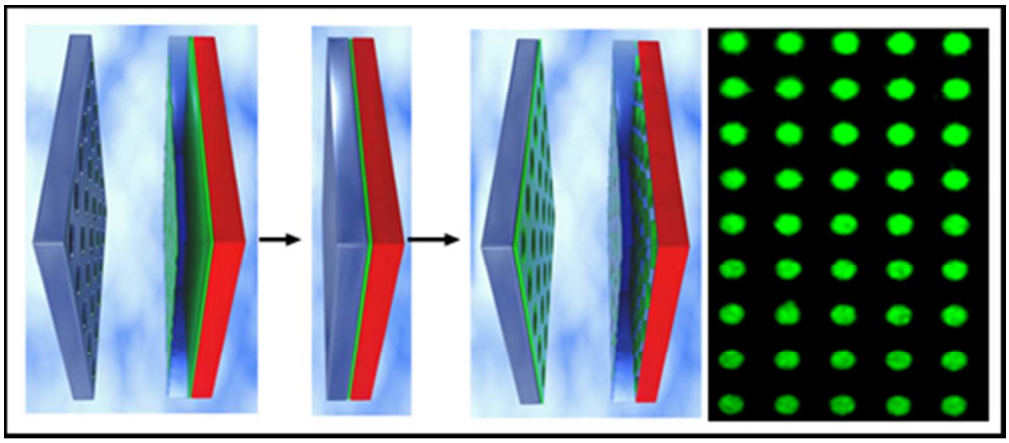

A theory and method for calculating printing resolution limits for microcontact printing of a condensed polyelectrolyte multilayer thin film, based on surface energies and line tension is presented.
176x76mm (72 x 72 DPI)

Cite this: DOI: 10.1039/c0xx00000x

www.rsc.org/xxxxxx

ARTICLE TYPE

Micro-Contact Printing of PEM Thin Films: Effect of Line Tension and Surface Energies

Meiyu Gai [a,b], Johannes Frueh[a]*, Agnes Girard-Egrot[c], Samuel Rebaud[c], Bastien Doumeche[c], Qiang He[a]*

Received (in XXX, XXX) Xth XXXXXXXXX 20XX, Accepted Xth XXXXXXXXX 20XX

DOI: 10.1039/b000000x

Polyelectrolyte multilayer (PEM) thin films are popular candidates for surface coating due to their versatility, tunability and simple production method. Often these films are used in a 2D structured manner for creating defined cell scaffolds or electronic applications. Although these films were successfully printed in the past, the conditions and energies necessary for a successful printing were only investigated as isolated parameters or as a function of the substrate but not the PEM surface energy and therefore the dominating forces remained controversial. We hereby present a theory and method for microcontact printing of condensed polyelectrolyte multilayer thin films, based on surface energies and the line tension. The theory relies on the surface energy of the substrate, stamp and PEM as well as the PEM line tension ratios to create the desired pattern. The presented theory is able to predict the printability, quality and resolution limit of a chosen system and was evaluated with experiments. A reduction of the production time from the beginning of PEM assembly to the final pattern from several hours down to 30 minutes was achieved while increasing reproducibility and resolution of the printed patterns at the same time. We would like to point out, that this approach can generally be used for any kind of adsorbed thin film on substrates.

Introduction

The creation of well-defined micro- and nanostructures is a prerequisite for a multitude of applications ranging from electronic circuits[1] over antibiofouling coatings[2] and optical devices[3] to drug delivery systems[4,5]. Due to the limits, high costs and high efforts of top down processes like area selective etching[6] or photolithography[7,8], which usually demand high equipment standards (e.g. clean room) and well trained staffs, cheap and simple bottom up approaches become more and more popular.[9] One of these bottom up approaches is microcontact printing (μCP).[1,10] Another bottom up technique is the layer-by-layer self-assembly technique, which is used for e.g. the production of polyelectrolyte multilayer[11,12] (PEM) thin films. These thin films comprise out of polyelectrolytes (PE) which are polymers that contain ionic groups. The formation of PEM is facilitated by adsorption of these charged PE, leading to a surface charge overcompensation.[11] This allows adsorption of oppositely charged PE from solution due to an alternating immersion of a substrate into solutions of oppositely charged PE.[13] The adsorption is based on electrostatic interactions, allowing materials like nanoparticles or even living cells, to be incorporated into these films.[13]

A combination of μCP and PEM thin films was first introduced 2004 by Park and Hammond printing PEM thin films deposited onto a silicone rubber stamp to glass slides, calling it "multilayer transfer printing".[14] Zhang et al on the contrary called it a "μCP method", while Shen and co-workers called it "lift off" method.[4,15,16] Although, this method is used for the creation of a multitude of structures intended from electrical circuits to drug delivery purposes, there is no unified theory or method how to perform the printing process or why it works.[15,17] Until now every publication focusing on this topic states different effects being responsible for the μCP of PEM leading to contradictory statements and results in literature.[14,15,18,19] Hammond and Park stated in their first publication electrostatic forces being the dominating effect, while they claimed hydrophobic forces being dominant in a subsequent publication.[14,19] The same team investigated also the transfer (printing) of single negatively charged Polyelectrolyte layers with resolutions down 80nm from a hard stamp to a PEM layer.[20] In their report, however, only the mechanical properties and surface energy of the stamp in relation to the stamp structural stability for such small patterns were investigated.[20] The fact that the PE layer on top has a different surface energy, which alters the system's surface energy was neglected.[20] An interesting and not answered question is why nanoparticle[16,21] and carbon nanotube[22] containing PEM films can be printed at all. This question arises since Zhang only focused on mechanical forces ignoring surface energy effects, claiming only soft films can be transferred, while Park claimed capillary forces being the only important parameter.[15,18]

Parallel to Hammonds multilayer transfer printing, which uses soft stamps and low pressures, an alternative approach using hard stamps, long term contact (3 to 24 hours) and high pressures (30-100 bar) which induces liquefaction of PEM films to let the film

"flow" into desired shapes of designed nanopatterns was developed by the Shen group.[16,23,24] This group reported a "lift off" PEM printing technique similar to the multilayer transfer printing technique of Hammond, stating that the necessary forces for the "lift off" of gold nanoparticle containing films are dispersion forces, however like in case of the Hammond group no calculation was shown.[16]

This paper presents a general theory and method of PEM μCP based on surface energies and line tensions, relying on the physical-chemical properties of a PEM staying in condensed state during the whole printing process. In addition a qualitative explanation is presented for special cases like PEM films being printed with stamps at temperatures surpassing the glass-transition temperature or transferring hard but brittle nanoparticle or carbon nanotube containing PEMs.

Materials, Methods and Theory

Materials

Silicone rubber (PDMS) (Sylgard 184, Dow Corning, Midland, MI) was used as a flexible low surface energy substrate for PEM production. The base (component A) and curing agent (component B) of the PDMS were mixed in a 10:1 ratio, degassed in vacuum for 30 minutes and cured for 3 hours at 70 °C.

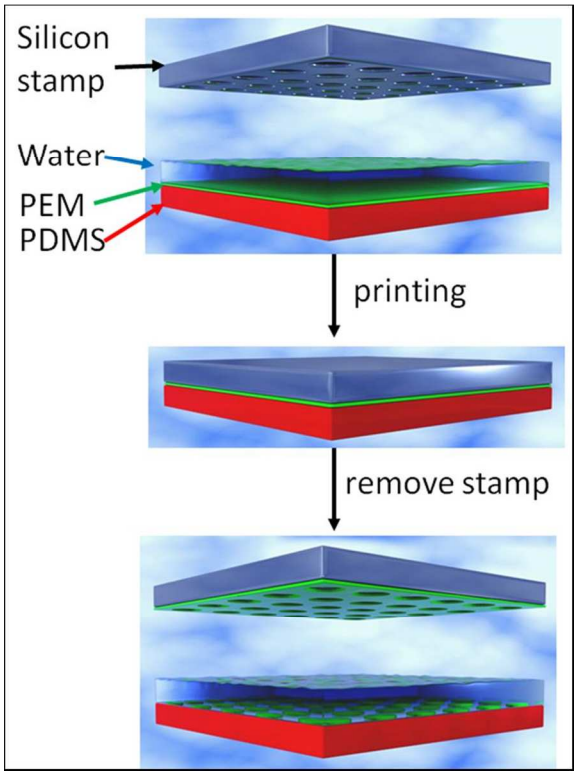

Fig. 1 Schematic representation of the printing process in wet (aqueous) condition. After assembling the PEM onto the PDMS substrate, the patterned silicon stamp was pressed with a force of 10-50 g/cm^2 onto the substrate for 5 s. Then the stamp was removed. The surface energy of the silicon stamp is significantly higher than the one of the PDMS, therefore the PEM touching the silicon master transfers to the silicon stamp. The PEM not touching the silicon stamp during printing, will stay on the PDMS, if the line tension of the PEM is lower than the PDMS surface energy.

The polyelectrolyte concentration was 0.5 g/L and the ionic strength (NaCl, Chemical Reagents, Tianjin, China) was 0.5 M. The spraying cans used were DC (Duennschicht Chromatographie) Spruehflaschen (type Air Boy, Nr. 0110.1) obtained from Carl Roth, Germany. The used polyelectrolytes and their molecular masses were poly(styrenesulphonate) (PSS) (molecular weight (MW) 70000 g/mol), poly(diallyldiammonium) chloride (PDDA) (MW 100000-200000 g/mol), poly(acrylic) acid (PAA) (MW 1800g/mol), poly(allylamine) hydrochloride (PAH) (MW 56000g/mol)) and poly(ethylenimine) (PEI) (MW ~750000 g/mol).

All polyelectrolytes mentioned above were purchased from Sigma-Aldrich (St. Louis, USA). PAHFITC represents fluorescein isothiocyanate (FITC) labelled PAH, whereby the FITC was bought from Sigma-Aldrich (St. Louis, USA). The FITC was linked to the PAH according to reference 25. The hPAA denotes PAA with a high molecular weight (240000 g/mol, 25 wt% in water, Alpha Aeasar, Tianjin, China). The used water was ultra-pure water (18.2 MΩcm) (Purelab Classic, Elga Lab water, Beijing, China). The PVA poly(vinylalkohol) was bought from Tianjin Basifu, Harbin, China. The polystyrene for the sacrificial layer was bought from Sigma (St. Louis, USA). The abbreviations in this publication are summarized in table 1.

Table 1. Used abbreviations in this publication

Abbreviation	Full name or Description
PEI	Poly(ethylenimine)
PSS	Poly(styrenesulphonate)
PDDA	Poly(diallyldiammonium) chloride
PAA	Poly(acrylic acid)
PAH	Poly(allylamine) hydrochloride
MW	Molecular weight
FITC	Fluorescein isothiocyanate
hPAA	High molecular weight PAA
PVA	Poly(vinylalkohol)
PolyS	Poly(styrene)
PEM	Polyelectrolyte multilayer
PDMS	Polydimethylsiloxane silicone rubber
PE	Polyelectrolyte
μCP	Microcontact printing
LbL	Layer-by-Layer
P_1	Printing parameter for PEM-stamp and PEM-substrate surface energy difference
P_2	Printing parameter for PEM-substrate surface energy and line tension energy difference
PS	PEM and stamp surface energy interaction
PP	PEM and substrate surface energy interaction
L	Line tension

P_3	L dependent printing parameter with P_1 being constant
λ	Buckling wavelength
h	Film height
v	Poisson Ratio
E_f	Elastic modulus of film
E_s	Elastic modulus of substrate
SIEBIMM	Strain induced elastic buckling in mechanical measurements

Methods

An inverse printing method is used in which a structured silicon stamp is directly pressed onto a PEM coated silicone rubber (PDMS) sheet. In current systems proposed until now usually a structured PDMS stamp coated with PEM is used.[4,15] The inverse printing (intended structures remain on PDMS, rest is lifted off similar to the "lift off" technique[16] but with more defined surface energies) method poses the advantage that the expensive silicon stamp cannot be contaminated with PDMS and is easily cleaned. The PEM on the PDMS was prepared by the layer-by-layer (LbL) spraying deposition method[26], which is a fast production method (6 s compared to 5 minutes for the dipping method for a monolayer). The PEM thin films spraying sequence (corresponding numbers are used as sample types in this paper) onto PDMS was:

1. $PEI(PSS\text{-}PDDA)_4(PSS\text{-}PAHFITC)_2$;
2. $PEI(PSS\text{-}PDDA)_4(PSS\text{-}PAHFITC)_2PSS$;
3. $PEI(PAA\text{-}PAH)_4(PAA\text{-}PAHFITC)_2$;
4. $PEI(PAA\text{-}PAH)_4(PAA\text{-}PAHFITC)_2PAA$;
5. $PAA\text{-}PAH\ (PSS\text{-}PDDA)_{10}(PAA\text{-}PAHFITC)_2$;
6. $PEI(hPAA\text{-}PAH)_4(hPAA\text{-}PAHFITC)_2$;
7. $PEI(PSS\text{-}PAHFITC)_2PSS\text{-}PDDA$;
8. $PEI(hPAA\text{-}PAHFITC)_2$

PEI was used in most of the samples as anchoring layer (first layer) on the PDMS due to its well-known sticking properties[27] and its ability to promote a positive surface charge on the uncharged PDMS. Sample 5 uses PAA as the initial layer to compare the results with reference 15. The denominators behind the brackets of the sample structures symbolize repetitions of bilayer groups.

In addition to the positive charge terminated samples 1, 3 and 5-8 also negative charge terminated samples 2 and 4 were prepared to examine the effect of terminal charge on the printing quality. Since polyelectrolytes are either positively or negatively charged, we could not investigate the validity of our approach for non-charged films. At this point we would like to point out, that our approach should also work for uncharged films e.g. hydrogen-bridge based films[28] as the printing is based only on surface force differences. In addition the substrate or stamp charge only affects the film printing quality in terms of surface energy strength. Therefore neutral materials can also be used as stamps and substrates especially since polyelectrolytes can also adsorb due to hydrophobic interactions.[27,29]

Samples 6-8 were produced to determine the influence of the line tension in relation to the elastic modulus (differences in molecular weight in sample 6 and 8) as well as bilayer number (variations of the bilayer number from 3.5 to 13 bilayers in case of sample 5 and 7) onto the printing quality.

The utilized silicon stamps had holes with diameters of 5 and 10 μm. The depths of these holes were 3 to 4 μm. The masks for these silicon stamps were produced by the Chinese academy of sciences (Beijing, China), whereby the patterning of the silicon stamps was done in Institute Nr. 49 at Harbin Institute of Technology (Harbin, China). In addition ring and line like patterns of length scales from 25 μm to 1 μm were printed with silicon stamps to determine the limit of reliable printing patterns for PEM. The size of all silicon stamps was 1x1 cm^2.

Printing of the patterns was performed under two different conditions for comparison reasons:

Condition one: After the PEM thin film was assembled onto the PDMS substrate, it was dried with N_2, the silicon stamp was pressed onto the PEM for 5 seconds, and then the silicon stamp was removed.

Condition two: After the PEM thin film was assembled onto the PDMS substrate, the silicon stamp was pressed onto the PEM in wet condition (thin water layer, caused by adding a drop of water onto the substrate, covering the PEM), as shown in Fig. 1. Printing pressures of 10, 20, and 50 g/cm^2 at 22 °C were used for wet and dry printing.

The resulting PEM patterns were investigated under an Olympus BX51 microscope in fluorescence mode. Scanning electron microscopic (SEM) images were obtained in case of a transfer from PDMS to gold coated silicon wafers for better contrast. The utilized SEM was a Helios NanoLab 600i (FEI, Hillsboro, Oregon, USA). For SEM measurements the PEM structures were printed onto a gold coated silicon wafer (sputter coated 8nm gold) for better contrast. The gold and silicon ensure a conductive substrate and a bright background with a dark PEM in the SEM image. Although gold is a non-charged substrate printing on it is no problem to print on it due to an overall high surface energy of the gold. Height measurements were obtained by using a Dimension Fast Scan atomic force microscope (AFM) (Brucker, Billerica, USA). The used AFM probe was a Brucker RESP-20 probe with a force constant of 0.9 N/m. The characterization was done in standard contact mode using the NanoScope software pre-set system. The height calibration of the NanoScope system was done using standard PEM samples with known height. These standard PEM samples had 16 bilayers of PSS and PDDA (produced by the same way as described above) whereby the thickness was known from X-ray and neutron reflectometry (measured at V6 in the Helmholtz Berlin).[30,31]

Production and dissolution of sacrificial layers

To release the PEM patterns from the PDMS substrates into solution, a sacrificial layer has to be used. PVA (polyvinylalkohol) was dissolved in hot water (98°C) (saturated solution) and spin-cast at 3000 rpm (rotations per minute) onto a clean glass slide (cleaned for 15 minutes with Pyranha solution (50 % concentrated (98 %, purity, p. a.)) H_2SO_4 and 50% H_2O_2 (30 %, purity, p.a.). *Since Pyranha solution is highly oxidizing and heat creating it is necessary to utilize this solution very carefully*. After printing the PEM patterns with afore mentioned methods, the PVA was dissolved in hot water to release the PEM patterns. Also PolyS (Polystyrene) was used as a sacrificial layer.

The PolyS was dissolved in Toluene (St. Louis, USA), as a saturated solution and the clean glass slides were dipped into solution and dried in a fume hood. After printing of the PEM patterns with afore mentioned method, the PolyS was dissolved in toluene to release the PEM patterns. Scheme S1 in the supporting information (SI) shows the release mechanism of PEM plates in dry and wet printing approach from sacrificial substrates.

Mechanical Measurements

The PEM elastic modulus which was utilized as the line tension was obtained from mechanical measurements utilizing SIEBIMM[32] measurements for wet (in water) and ambient (dry, 17% relative humidity, 20°C) conditions. The values were obtained from references as well as own measurements. For the mechanical measurements, the PEM was clamped into a home-made stretching device (shown in Figure S1 SI). The degree of elongation was 10%. Upon release the wrinkling wavelength was determined by static light scattering (laser wavelength 532nm) and microscopic observations. The elastic modulus was determined with following equation[32,33]

$$\lambda = 2\pi h^3(((1-v^2)E_f)/((1-v^2)3E_S) \quad (1)$$

Here λ is the buckling wavelength, v the Poisson ratio (0.5 assumed) and E the Young's modulus. The subscripts f and S symbolize film (PEM) and substrate (PDMS) respectively. The Young's modulus was taken as the line tension in this work.

Theory

The PEM printing, if one considers only the surface energies in two and one dimensions, depends on the PEM-substrate (PP) interaction, the PEM-stamp (PS) interaction and the PEM cohesion energy (L) (line tension, of the PEM line which needs to be ripped for the printing pattern structure). The surface energy properties and used values are explained in detail below and in the supporting information.

From these energies printing parameters (P) were derived, which show positive values in (2 a) and (2 b) for the possibility of a successful printing of the PEM. Negative values in one or both of the two equations result in a failure of the printing process (see equation 2 a and b).

$$P_1 = (PS - PP) \quad (2\text{ a})$$

$$P_2 = (PP - L) \quad (2\text{ b})$$

Please note, that PP in case of (2 b) is the PEM-stamp interaction energy of the PEM pattern area while L is the length around the pattern. In (2 a) normalized values for PS and PP, as well as pattern areas can be used due to this equation being of comparative nature.

If only the possibility of printing for different structure sizes (e.g. up to which size can be printed) is of interest, and $P_1>0$ then P_1 can be considered being a constant for P_2. In this case P_2 is the variable because L and PS change with the size of the printed features, whereby P_1 also changes, but never changes the prefix. The point at which the prefix of P_2 changes is the point above which the structures can be reasonable be printed. This limit can therefore be determined either solely with equation (2 b) or equation (3).

$$P_3 = P_1 \cdot P_2 \quad (3)$$

In P_3 only the sign is of binary significance (positive = printable, negative = not). The values themselves are not stating physical values.

In equation 2 and 3 surface energy values are used for PS and PP. It is important to note, that always the component with the weaker surface energy is the one defining the surface interaction strength. It is also important that the components of the surface energy interact with the relevant component of the surface energy, e.g. surfaces with polar or ionic components will not interact much with unpolar components.[34] Table S1 shows the surface energy values used in equation 2 and 3 in this study. The values in Table S1 are mainly from literature.[35,36,37,38,39,40–42] SI page 6-9 explains the measurement methods used in the corresponding literature along with the determination and calculations performed by the authors of this study for the ionic component of the surface energy of PEM.

Results and Discussion

Mechanical measurement results: The PSS-PDDA film is in wet condition too soft or too thin to form wrinkles on PDMS. This is because the total mechanical strength of the elongated PSS-PDDA film is too low to deform the underlying PDMS. Such a finding is in agreement with earlier observations.[32] For this reason the value of PSS-PDDA in wet condition in Table S 2 shows the minimum measurable value of the measurement method in the presented system. The obtained mechanical values for wet PEM lie in the range of rubber but are still much higher than those of PDMS used as supports for the measurements. Note that depending on curing conditions, temperature and age, the elastic modulus of PDMS can vary from 0.1 MPa to far above 10 MPa[43,44]. The obtained values are in agreement with mechanical measurements made by compressing PEM capsules, where the PEM mechanical properties were tuned with the bilayer numbers (elastic modulus between 500 kPa and 61 MPa, depending on shrunk or pristine capsules).[45] It is also noted, that these films are much harder than poly(L-lysine) and hyaluronic acid films, which exhibit an elastic modulus of ~80 kPa.[46] The dry films exhibit a much higher elastic modulus of 1 and 10 GPa for the PSS-PDDA and PAA-PAH film (see Table S 2).

In equation (2 a) and (2 b) PP is defined as the surface energy which interacts between the PEM and the substrate (here PDMS). The PDMS surface energy is much lower than that of the PEM. Therefore PP is clearly dominated by the low energy of the PDMS, and therefore the PDMS surface energy[47,48] is used to describe the PP interaction. On the contrary the utilized stamp material (silicon) has a higher ionic, polar and dispersion surface energy than the PEM. Therefore the PEM defines the PEM-stamp (PS) interaction. In this case care has to be taken which charge types are present on the surfaces. Since the silicon surface charge is negative, positively charge terminated PEM interacts more with silicon than negative charge terminated ones.

Since the used PEM types in our own experiments presented in this study all result into a $P_1 >0$ we show in Fig 2 for the two investigated structure sizes P_3 to emphasize the change in printability for sample type 2 and 5 as a function of the printed pattern structure compared to the other samples. This dependence on the printed structure size is because of the line tension which strongly depends on the mechanical properties of the PEM. P_2 not only depends on L but also on the PEM-stamp interaction PS, whereby PS increases with increasing printing pattern size as a

square of the structure radius, while L only increases linearly. Therefore P_2 becomes more positive with increasing pattern size.

Depending on the relative interaction strengths between PP, PS and L as stated in equations 2a and 2b, three scenarios are plausible:

1) If the PEM-substrate interaction PP is larger than the PEM-stamp interaction PS, the PEM will stay on the substrate. In this case L does not matter.

2) If the PEM substrate interaction PP is smaller than the PEM-stamp interaction PS and L is larger than the PEM-substrate interaction PP, a complete transfer of the PEM from the substrate to the stamp will occur.

3) If the PEM-substrate interaction PP is smaller than the PEM-stamp interaction PS and L is smaller than the PEM-substrate interaction PP, the pattern of the stamp will be reproduced with the printed PEM.

Minimum printing pattern size: Using equation 3, for circular patterns with diameters ranging from 2.5 to 10 µm for PEM types 1-5, one obtains a clear discrepancy between dry and wet printing due to differences in L as shown in Fig. 2 A-D (for 5 and 10 µm) and Fig. S 2 (for plates with a diameter of 2.5 µm). As a result of the large L in dry condition (Fig 2 A and C), printing of dry PEM is not possible for all investigated pattern sizes. This can be seen clearly in the negative P_3 for dry conditions in Fig. 2 B and D. Surprisingly, a complete transfer of the PEM to the silicon stamp was not observed experimentally, probably due to low contact regions (nanoroughness) which is probably decreased by PEM swelling in wet conditions.

Printing the same PEM in wet conditions (>90% r.H. (relative humidity) or directly in water) resulted for structures above ~5 µm in printed patterns for the positively terminated PEM types used. The PEM line tension is very close to the PEM-substrate interaction PP for plates with a diameter of 5 µm. This suggests that frequent printing errors might occur, which were indeed confirmed experimentally by PEM remaining on the PDMS as well as on the PEM transferred to the wafer (see imperfect borders of the structures in Fig. 3 A-C). This case is a good example of the third printing case: reproduction of the stamp patterns.

For plates with a diameter of 2.5 µm, no printing is according to our theory possible, as can be seen in SI Fig. S2. This result was confirmed experimentally, although variations were observed which are discussed in the later sections.

Sacrificial substrates: Due to the higher surface energy of sacrificial substrates compared to PDMS, the PEM patterns can easily be transferred to a sacrificial substrate and also be brought to solution where they don't fold, due to self-repulsion of the positive surface charges in case of sample type 3. The self-repulsion effect is caused by the excess of positively charged polyelectrolytes inside of the PEM.[49–51] Fig. 3 B and D show such plates on PVA and released in solution.

Hydrophobic and low energy substrates: In the special case of using a hydrophobic substrate (e.g. Teflon) coated with a film and utilizing a stamp with high surface energy, significantly larger pattern areas are needed to prevent a complete lift off as well as to be able to overcome the line tension of the structures, see SI Fig. S 3 for such an example.

Printing efficiency and quality of the wet printing process: For sample type 1 at 22 °C and 50 g/cm^2 pressure a success rate of ~5% was achieved, which is quite low. At other pressures the success rate was close to 0. This proves a low PEM-stamp (PS) interaction energy and high L. This is because the PDDA surface energy is lower compared to e.g. PAH surface energy. For sample type 3 the success rate was for all observed pressures much higher, for 50 and 20g/cm^2 close to 95% and for 10g/cm^2 close to 50%. This is due to high PEM-stamp (PS) interaction energy and L being lower than the PEM-substrate interaction energy (PP). Sample type 6 showed a similar success rate like sample type 3, with the difference that large chunks were ripped out, proving high PEM-stamp (PS) interaction energy and a high L. Sample 7 showed patterns comparable to sample 3 proving that a decrease in bilayer number (PEM thickness) decreases L, leading to better structures, while keeping the same molecular structure and surface energy (PS).

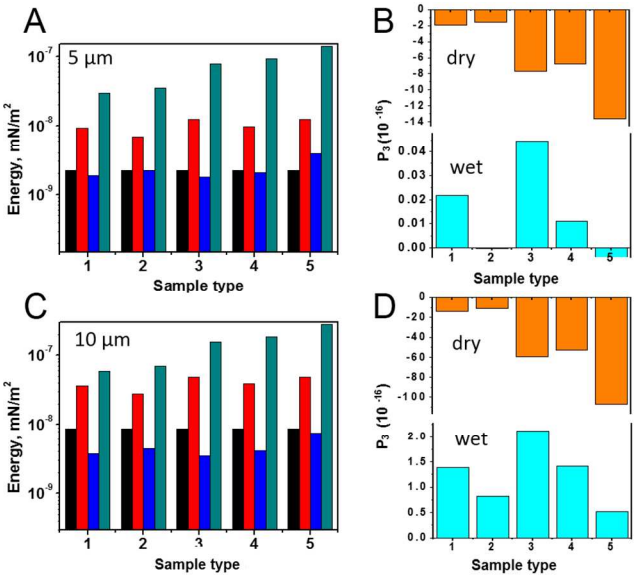

Fig. 2 Surface energies for 5 µm circular patterns (A) black is PS (PEM-stamp surface energy), red is PP (PEM-substrate surface energy), blue are wet and green dry values for L (line tension). The printing parameter in (B) shows the printability of (A) with orange being the printing parameter P_3 for dry and blue for wet conditions. 10 µm dot patterns (C) are able to print more PEM sample types like sample type 2 and 5 as P_3 in (D) shows.

Effect of pressure based decrease of L: The films of sample 3 and 7 showed for structures larger than 2.5 µm clear borders see Fig. 4 for fluorescence microscopic images and SI Fig. S 4 for AFM (atomic force) and SEM (scanning electron) micrographs. These findings are surprising; since equations (2 a), (2 b) and (3) forecast that the PEM thin film should not rip, at printing pattern sizes below 5 to 10 µm (depending on the sample type). This effect can be explained with the fact, that the PEM thin film partially experiences a glass-viscous flow transition[52,53] due to the mechanical pressure. Therefore the energy needed to rip the PEM thin film is lower than the one obtained from SIEBIMM[32] (wrinkle and laser based indirect mechanical thin film measurement technique) or AFM pressure measurements[45,54] which were used in the calculations. Another possibility explaining the discrepancy between the theoretical and practical minimum printing size stems from the fact, that the Young's moduli of the wet printed samples were close to the SIEBIMM resolution limit and therefore the real mechanical values were

slightly overestimated. Most likely both explanations sum up, affecting the differences between the experimental and theoretical printing pattern limit therefore being cumulative. Although the theoretical error is relatively small it is noteworthy.

Effect of printing pattern shape: Similar resolution limits were found for different PEM structures like stripes or ring structures as shown in Fig. 4. It is noted, that released, free standing films, exhibited the same structural features and resolution limits like the films on substrates.

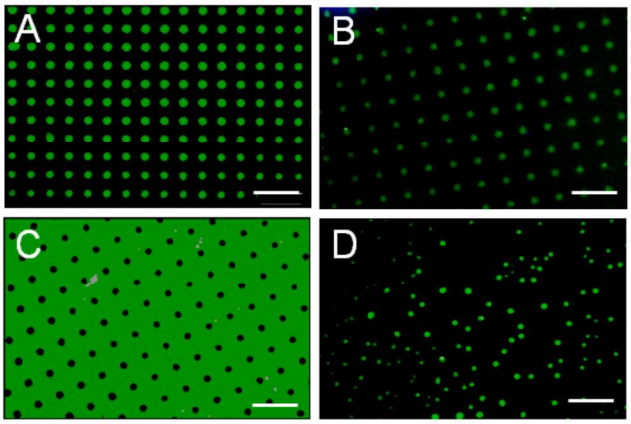

Fig. 3 Printing results of a PEI(PAA-PAH)$_4$(PAA-PAHFITC)$_2$ film. PEM on the PDMS side after printing with a silicon stamp (A) and on PVA (after transferring (A) to PVA) (B), the silicon stamp side (C), and released plates after dissolving the PVA sacrificial layer (D). Scale bar is 20 µm.

Effect of molecular weight: Interestingly the printing quality but not the efficiency for sample 8 is worse than for sample 7 and 3, which is due to the high L of this sample, stemming from the higher molecular weight of the used hPAA. The ripping on the borders is in many cases not complete and the minimum structure size is 3 to 5 times larger is than for sample 7 or 3. Images of these samples can be observed in SI Fig. S5 A-D. The high molecular weight was found to increase the Young's modulus of the PEM, which in turn increases L. A PAH-PAA bi-layer has for low molecular weight PAA a Young's modulus of 49MPa, while that of high molecular weight PAA (hPAA) has 129MPa. Therefore the minimum printing pattern size differs by factor ~3 and the printing quality and resolution is significantly better for low molecular weight PAA.

Effect of surface charge: According to our theory, only the positive charge terminated PEM films can be printed successfully, due to the higher PEM-stamp (PS) interaction compared to negatively charge terminated PEM films. This charge based effect was confirmed in experiments with negative charge terminated PEM films of sample 2 and 4 which could not be printed. Contrary to the theory, which forecasted case one, the negative charge terminated films were stuck within the silicon stamp holes for dry printing, and smeared on the silicon stamp for wet printing. This effect was seldom observed in case of positive charge terminated PEM films. This observation is attributed to glass-viscous flow transition effects, not covered by this theory. These glass-viscous flow transition effects can be conveniently minimized by decreasing the temperature or decreasing the printing pressure.[53]

Comparison of the theory with literature

The work by Zhang et al[15] investigated the printing effect of PEM films with different mechanical properties (L) can be explained well with equations (2 a) and (2 b), since the PEM film used by Zhang is thin and soft. The surface energies of the substrates used by Zhang are also agreeing with the requirement of equation (2 a). Zhang only investigated the mechanical properties of the released particles; the work stated no effect of the mechanical properties of on the printing quality, in comparison to our study. The work from Hammond[14,20] fits also very well into our model, when comparing the used PEM surface energy and line tension (L).

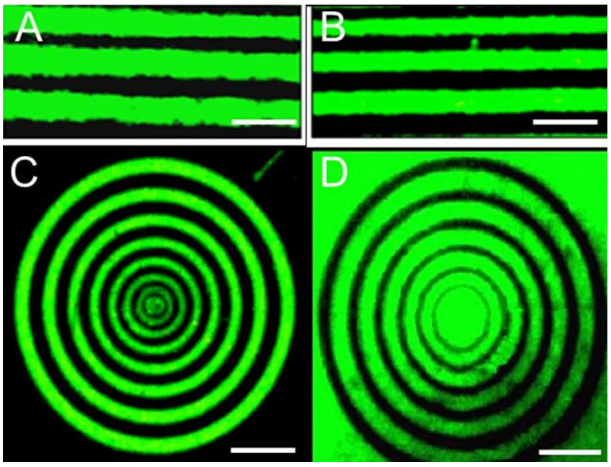

Fig. 4 Comparison of different printed PEM structures on silicon stamp and PDMS substrate after printing. (A) PEM lines on the silicon stamp (B) PEM lines remaining on PDMS after printing (C) PEM circles on the silicon stamp (D) PEM circles remaining on the PDMS. Scale bar is 20 µm.

The claim of reference 14 that only the ionic part of the surface energy (precisely PS was discussed only) is important, contradicts the claim of reference 20 discussing only the importance of the dispersion part of the surface energy (PS was the matter of discussion in 20). In reality both energies in addition with the dipole part of the surface energy are important[34], and hence for the printing quality. The reason that reference 14 and 20 report contradictory theoretical results is because they discuss isolated surface energy parameters.

The work from Shen's group[16,24] as well as reports of particle containing PEM films[16,21] being printable seem to disagree with our equations, since the line tension L of these films is in the range of many GPA[55,56]. In case of transferred PEM films containing particles it is necessary to take the brittleness of these films into account, since these films were in case of reference 22 printed with a flexible PDMS stamp at "several bars" for several hours and at large pattern sizes (100 x 200 µm²). Carbon nanotube containing PEM films break at ambient conditions at elongations >1%[55] which can be easily surpassed due to the PDMS stamp sideward buckling[43] at high pressures. For this reason the energy to surpass the line tension was delivered by the printing pressure and not by the surface energy of PS or PP.

For the system of Shen in reference 16, who successfully printed a gold-PEM composite film using the "lift off" method the stamp deformation cannot be used as explanation, since the film was already flat. The compression force in his case caused a liquefaction of the PEM composite below the stamp due to the

strong pressure (30 Bar) that makes L in this case obsolete. The statement of the authors of reference 16, that the photopolymer has a stronger dispersion interaction than a freshly cleaned glass slide is surprising, since most literature states at least three times higher values for glass than for polymers (see Table S1 in SI). Our interpretation for the observation in reference 16 is therefore, that the polymer surface softened alongside with the PEM on the given pressure, decreasing L. Our theory is supported by reports that PAA-PAH films usually soften at temperatures >120 °C[57] which is far higher than the reported 55 °C[20] for the used photopolymer. Therefore inter-diffusion of the photopolymer with the PEM and therefore increased sticking/mixing to the PEM especially (increasing the PS value). The slow removal process in reference 16 facilitated sufficient cooling allowed the stamp and PEM to harden out upon removal. This led most likely to this surprising effect.

Conclusions

In summary, the presented novel theory and optimized μCP method of PEM, based on surface- and line tension, opens up the possibility to print faster and more reliable PEM thin films. The time from PEM film production to printed structures which lasted in the past 16 hours like in reference[15] or 4-5 hrs like in reference[14] was decreased to 30 minutes (if PDMS substrates are present), by preventing failures due to drying at the same time. The presented theory is able to explain all not melting based PEM printing results published until now.

The reports, size and printing quality of printed patterns published by Park, Hammond and Zhang fit well with the presented theory.[14,15,18,19] It also unifies the surface, mechanical and charge effects which were in the past only investigated as single parameters.[14,15,18,19] The presented printing parameters allow a simple and fast estimation of the printing limit, and printing possibility.

The PEM melting and glass-viscous flow transition[53] properties need to be considered in μCP as well, but can be minimized with the proper choice of temperature and printing pressure. With this optimized method, PEM printed patterns can now be utilized for a more reliable production of defined and smaller patterns (sub μm[1,58] in case of very soft PEM films, or even in the range of nm in case of PEM in viscous flow state[24,53]). This is important for electronic, optical and drug delivery applications. Due to the effect being limited by line tension, super-hard thin films based on graphene or carbon-nanotubes, are not printable directly with this method, however PDMS buckling due to pressure (external energy delivery to overcome the line tension) as well as other effects (e.g. like temperature or pressure based film softening) can ensure a successful print.[55,59,60]

It is important to note, that the presented equations and functions are extendable to other kinds of thin adsorbed films, since the equations and surface force effects are general.

Acknowledgements

The authors would like to thank China Postdoctoral Science Foundation (2013M531019), HIT start-up grant, EU-FP7 BIOMIMEM staff exchange project, Chinese Scholarship Council (201406120038), Queen Mary University of London, for funding this research and Lars Woerner for rendering the schemes. In addition the authors would like to thank Dr. Ralf Koehler for help and discussions and the Helmholtz Center Berlin for Neutron and X-ray data of the AFM calibration sample.

Notes and references

[a] *Key Laboratory of Microsystems and Microstructures Manufacturing, Micro/Nano Technology Research Centre, Harbin Institute of Technology, Yikuang Street 2, Harbin 150080, China. Fax: :+86045186403605; E-mail: Johannes.Frueh@hit.edu.cn; Qianghe@hit.edu.cn*

[b] *Queen Mary University of London, Mile End, Eng, 215, London E1 4NS, United Kingdom.*

[c] *Institut de Chimie et Biochimie Moléculaires et Supramoléculaires, Universite Claude Bernard Lyon 1, 43 boulevard du 11 Novembre 1918 F-69622 Villeurbanne cedex, France.*

† Electronic Supplementary Information (ESI) available: See DOI: 10.1039/b000000x/

1 H. A. Biebuyck, N. B. Larsen, E. Delamarche and B. Miche, *IBM J. RES. Dev.*, 1997, **41**, 159–170.
2 J. Frueh, M. Gai, Z. Yang and Q. He, *J. Nanosci. Nanotechnol.*, 2014, **14**, 4341–4350.
3 M. Pretzl, C. Hanske, A. Chiche, U. Zettl, A. Horn, A. Böker, A. Fery and A. Schweikart, *Langmuir*, 2008, **24**, 12748–12753.
4 P. Zhang, Y. Liu, J. Xia, Z. Wang, B. Kirkland and J. Guan, *Adv. Healthc. Mater.*, 2013, **2**, 540–5.
5 D. V Volodkin, A. I. Petrov, M. Prevot and G. B. Sukhorukov, *Langmuir*, 2004, **20**, 3398–406.
6 C. Ebert, J. Levkoff, J. Roberts, J. Seiler, C. Wanamaker and T. Pinnington, *J. Cryst. Growth*, 2007, **298**, 94–97.
7 F. Rehfeldt and M. Tanaka, *Langmuir*, 2003, 1467–1473.
8 T. Fujigaya, S. Haraguchi, T. Fukumaru and N. Nakashima, *Adv. Mater.*, 2008, **20**, 2151–2155.
9 K. Kim, X. Xu, J. Guo and D. L. Fan, *Nat. Commun.*, 2014, **5**, 3632.
10 C. Y. Hui, A. Jagota, Y. Y. Lin and E. J. Kramer, *Langmuir*, 2002, **18**, 1394–1407.
11 G. Decher, J. D. Hong and J. Schmitt, *Thin Solid Films*, 1992, **210-211**, 831–835.
12 G. Decher, *Science (80-.).*, 1997, **277**, 1232–1237.
13 G. Decher and J. Schlenoff, *Multilayer Thin Films: Sequential Assembly of Nanocomposite Materials*, Wiley-VCH Verlag GmbH & Co. KGaA, Weinheim, 2nd edn., 2012.
14 J. Park and P. T. Hammond, *Adv. Mater.*, 2004, **16**, 520–525.
15 P. Zhang and J. Guan, *Small*, 2011, **7**, 2998–3004.
16 X. Chen, J. Sun and J. Shen, *Langmuir*, 2009, **25**, 3316–3320.
17 F. Basarir, *ACS Appl. Mater. Interfaces*, 2012, **4**, 1324–9.
18 J. S. Park, S. M. Cho, G. Y. Han, S. J. Sim, J. Park and P. J. Yoo, *Langmuir*, 2009, **25**, 2575–81.
19 J. Park, L. D. Fouché and P. T. Hammond, *Adv. Mater.*, 2005, **17**, 2575–2579.
20 J. Park, Y. S. Kim and P. T. Hammond, *Nano Lett.*, 2005, **5**, 1347–1350.
21 F. Ç. Cebeci, D. J. Schmidt and P. T. Hammond, *ACS Appl. Mater. Interfaces*, 2014, **6**, 20519–23.
22 B.-S. Kim, S. W. Lee, H. Yoon, M. S. Strano, Y. Shao-Horn and P. T. Hammond, *Chem. Mater.*, 2010, **22**, 4791–4797.
23 Y. Lu, W. Hu, Y. Ma, L. Zhang, J. Sun, N. Lu and J. Shen, *Macromol. Rapid Commun.*, 2006, **27**, 505–510.
24 Y. Lu, X. Chen, W. Hu, N. Lu, J. Sun and J. Shen, *Langmuir*, 2007, **23**, 3254–3259.
25 N. Kato and F. Caruso, *J. Phys. Chem. B*, 2005, **109**, 19604–12.
26 J. B. Schlenoff, S. T. Dubas and T. Farhat, *Langmuir*, 2000, **16**, 9968–9969.

27 J. Frueh, G. Reiter, H. Möhwald, Q. He and R. Krastev, *Colloid Surf. A*, 2012, **415**, 366–373.
28 a V Ermoshkin, a N. Kudlay and M. Olvera de la Cruz, *J. Chem. Phys.*, 2004, **120**, 11930–40.
29 J. Park and P. T. Hammond, *Macromolecules*, 2005, **38**, 10542–10550.
30 J. Früh, A. Rühm, H. Möhwald, R. Krastev and R. Köhler, *Phys. B*, 2015, **457**, 202–211.
31 L. G. Parratt, *Phys. Rev.*, 1954, **95**, 359–369.
32 A. J. Nolte, M. F. Rubner and R. E. Cohen, *Macromolecules*, 2005, **38**, 5367–5370.
33 A. L. Volynskii, S. Bazhenov, O. V Lebedeva and N. F. Bakeev, *J. Mater. Sci.*, 2000, **35**, 547–554.
34 C. J. V. a N. Oss, R. J. Good, C. J. Van Oss and M. K. Chaudhury, *Chem. Rev.*, 1988, **88**, 927–941.
35 Quest@surface-tension.de, *Internet*.
36 K. K. Lee, B. Bhushan and D. Hanford, The Ohio State University, 2005.
37 R. J. Jaccodine, *J. Electrochem. Soc.*, 1963, **110**, 524.
38 J. C. Joud, C. Vittoz and P. E. Dubois, in *Proc. Int. Conf. High Temperature Capillarity 29 June – 2 July 1997, Cracow, Poland*, ed. N. E. and N. Sobczak, Instytut Odlewnictwa, Cracow, 1997, pp. 167–174.
39 M. N. Hamblin, J. M. Edwards, M. L. Lee, A. T. Woolley and A. R. Hawkins, *Biomicrofluidics*, 2007, **1**, 34101.
40 M. Kolasiska, Polish Academy of Sciences, 2006.
41 G. Jiang, S.-H. Min and S. K. Hahn, *Biotechnol. Bioprocess Eng.*, 2007, **12**, 684–689.
42 T. Radeva, *Physical Chemistry of Polyelectrolytes*, M. Dekker, New York, 2001.
43 K. G. Sharp, G. S. Blackman, N. J. Glassmaker, A. Jagota and C.-Y. Hui, *Langmuir*, 2004, **20**, 6430–8.
44 A. J. Nolte, N. D. Treat, R. E. Cohen and M. F. Rubner, *Macromolecules*, 2008, **41**, 5793–5798.
45 M. Delcea, S. Schmidt, R. Palankar, P. A. L. . Fernandes, A. Fery, H. Möhwald and A. G. Skirtach, *small*, 2010, **6**, 2858–2862.
46 S. Schmidt, N. Madaboosi, K. Uhlig, D. Köhler, A. Skirtach, C. Duschl, H. Möhwald and D. V. Volodkin, *Langmuir*, 2012, **28**, 7249–7257.
47 J. C. Agar, K. J. Lin, R. Zhang, J. Durden, K. Moon, C. P. Wong and F. Drive, *Novel PDMS (silicone)-in-PDMS (silicone): Low Cost Flexible Electronics without Metallization*, Atlanta, 2010.
48 M. Salta, J. a Wharton, P. Stoodley, S. P. Dennington, L. R. Goodes, S. Werwinski, U. Mart, R. J. K. Wood and K. R. Stokes, *Philos T Roy Soc A*, 2010, **368**, 4729–54.
49 R. a Ghostine, M. Z. Markarian and J. B. Schlenoff, *J. Am. Chem. Soc.*, 2013, **135**, 7636–46.
50 R. v. Klitzing, *Phys. Chem. Chem. Phys.*, 2006, **8**, 5012–5033.
51 K. Köhler, P. Biesheuvel, R. Weinkamer, H. Möhwald and G. Sukhorukov, *Phys. Rev. Lett.*, 2006, **97**, 3–6.
52 J. Frueh, G. Reiter, H. Moehwald, Q. He and R. Krastev, *Phys. Chem. Chem. Phys.*, 2013, **15**, 483–488.
53 M. Gai, J. Frueh, G. Sukhorukov, A. Girard-Egrot, S. Rebaud, B. Doumeche and Q. He, *Colloid Surf. A*, 2015, **asap**, DOI: 10.1016/j.colsurfa.2015.05.009.
54 R. Mueller, K. Koehler, R. Weinkamer, G. Sukhorukov and A. Fery, *Macromolecules*, 2005, **38**, 9766–9771.
55 A. A. Mamedov, N. A. Kotov, M. Prato, D. M. Guldi, J. P. Wicksted and A. Hirsch, *Nat. Mater.*, 2002, **1**, 190 – 194.
56 J. Frueh, N. Nakashima, Q. He and H. Moehwald, *J Phys Chem B*, 2012, **116**, 12257–12262.
57 Q. He, W. Song, H. Moehwald and J. Li, *Langmuir*, 2008, **24**, 5508–5513.
58 E. Delamarche, C. Donzel, F. S. Kamounah, H. Wolf, M. Geissler, R. Stutz, P. Schmidt-winkel and B. Michel, *Langmuir*, 2004, **19**, 8749–8758.
59 M. K. Gheith, V. A. Sinani, J. P. Wicksted, R. L. Matts and N. A. Kotov, *Adv. Mater.*, 2005, **17**, 2663–2670.
60 Q. Cheng, L. Jiang and Z. Tang, *Acc. Chem. Res.*, 2014, **47**, 1256–1266.